Iran. J. Radiat. Res., 2012; 10(2): 73-81

A fast model for prediction of respiratory lung motion for image-guided radiotherapy: A feasibility study

M. Zehtabian[1], R. Faghihi[1], M.A. Mosleh-Shirazi[2*], A.R. Shakibafard[3], M. Mohammadi[4], M. Baradaran-Ghahfarokhi[5]

[1]Medical Radiation Department and Medical Imaging Research Center, School of Engineering, Shiraz University, Shiraz, Iran
[2]Center for Research in Medical Physics and Biomedical Engineering and Physics Unit, Radiotherapy Department, Namazi Hospital, Shiraz University of Medical Sciences, Shiraz, Iran
[3]Radiology Department, Shiraz University of Medical Sciences, Shiraz, Iran
[4]Medical Physics Department, Royal Adelaide Hospital, Adelaide, Australia
[5]Medical Physics and Medical Engineering Department, School of Medicine, Isfahan University of Medical Sciences, Isfahan, Iran

Background: The aim of this work was to study the feasibility of constructing a fast thorax model suitable for simulating lung motion due to respiration using only one CT dataset. ***Materials and Methods:*** For each of six patients with different thorax sizes, two sets of CT images were obtained in single-breath-hold inhale and exhale stages in the supine position. The CT images were then analyzed by measurements of the displacements due to respiration in the thorax region. Lung and thorax were 3D reconstructed and then transferred to the ABAQUS software for biomechanical fast finite element (FFE) modeling. The FFE model parameters were tuned based on three of the patients, and then was tested in a predictive mode for the remaining patients to predict lung and thorax motion and deformation following respiration. ***Results:*** Starting from end-exhale stage, the model, tuned for a patient created lung wall motion at end-inhale stage that matched the measurements for that patient within 1 mm (its limit of accuracy). In the predictive mode, the mean discrepancy between the imaged landmarks and those predicted by the model (formed from averaged data of two patients) was 4.2 mm. The average computation time in the fast predictive mode was 89 sec. ***Conclusion:*** Fast prediction of approximate, lung and thorax shapes in the respiratory cycle has been feasible due to the linear elastic material approximation, used in the FFE model. **Iran. J. Radiat. Res., 2012; 10(2): 73-81**

Keywords: *Finite element modeling, lung motion, image-guided radiotherapy.*

INTRODUCTION

The goal of radiation therapy is to deliver a high dose to the tumor accurately while sparing normal tissues. For this reason, before irradiation, 3D images are provided to identify the tumor and organs at risk. The main problem occurs when we are faced with tumors moving during the irradiation period. In the lungs, because of the respiratory motion, tumor mobility can be as much as 4.5 cm [(1)]. Therefore, lung tumors and organs at risk often move by centimeters, confining efforts to escalate the delivered dose to the tumor to increase tumor control [(2, 3)].

Although many attempts have been made to overcome this problem and methods like breath-hold techniques, real-time tumor tracking, and respiratory gating have been introduced to account for respiratory motion, limited knowledge regarding both respiratory dynamics and prediction of localized deformation of the tumor hinder the usefulness of these methods. Therefore, to meet these two challenges, it is essential to study the lung motion process using computer-aided modeling of the respiratory cycle to allow the precision of the treatment to be improved. The effectiveness of the radiation treatment can be significantly

Corresponding author:
Dr. Mohammad Amin Mosleh-Shirazi, Physics Unit, Radiotherapy Department, Namazi Hospital, Shiraz University of Medical Sciences, Shiraz 71936-13311, Iran.
Fax: *+98 711 6474320*
E-mail: *amosleh@sums.ac.ir*

increased when the movement of the lung and the tumor can be predicted in a short time, and ultimately in real-time.

The finite element (FE) method offers the ability to predict spatial and temporal variations in organs, strain, and contact area/forces [4]. There has been an extensive amount of research regarding the benefits of biomechanical modeling, specially FE in surgical simulation, specifically for modeling brain and breast deformation [5, 6]. Most studies have mainly focused on single organ deformable registration [7-12]. Only limited investigations have been reported [13-14] regading the potential of applying FE to radiotherapy.

All of the studies mentioned above emphasized the importance of realistic tissue properties in their work and few incorporated precise organ anatomical details and boundary conditions in their models. However, no prior work has focused on fast 3D simulation of deformation of the thorax region due to respiration for image-guided radiation therapy (IGRT) applications.

In this work, a 3D FE method was used to model the specific geometry and simulate the interactions between the lungs and adjacent thorax structures. This approach can potentially predict the movement of the lungs, based on a single geometric model (derived from a planning or on-treatment CT dataset), using just the geometry as input. Our methodology is based on the reported work in Ref 13. The aim of this paper is to introduce this approach and test the feasibility of the model to predict respiratory lung deformation with a short computation time.

MATERIALS AND METHODS

Six CT datasets corresponding to six men were processed. Table 1 illustrates the patients' characteristics. All of the patients had a normal lungs with no breathing problems.

CT Imaging

The study protocol was approved by the Radiology Department at Shiraz University of Medical Sciences. For each patient, two sets of CT images were acquired and reconstructed on a Lightspeed VCT scanner (GE Medical Systems, USA) were obtained in single-breath-hold inhalation and exhalation stages in the supine position. Figure 1 illustrates the lateral topograms of a patient in inhalation and exhalation stages. The CT images were initially acquired using a separate program and then imported into ADVANTAGE WORK STATION V.4.3 (GE Medical Systems) for the measurements of

Table 1. Patients characteristics.

Characteristic	Mean (Range)
Age (years)	48.8 (36.0- 64.0)
Weight (kg)	69.5 (61.0- 78.0)
Maximal anterior-posterior dimension in inhale stage within the lung CT slices (mm)	187.1 (177.6-189.3)
Maximal anterior-posterior dimension in exhale stage within the lung CT slices (mm)	178.5 (167.8-179.8)
Maximal lateral dimension in inhale stage within the lung CT slices (mm)	248.2 (241.7-251.1)
Maximal lateral dimension in exhale stage within the lung CT slices (mm)	237.1 (230.7-239.2)

the displacement due to respiration in the thorax region. A radiologist expert in CT image interpretation reviewed all imaging sets. For each image, the thorax region was outlined at inhalation relative to exhalation.

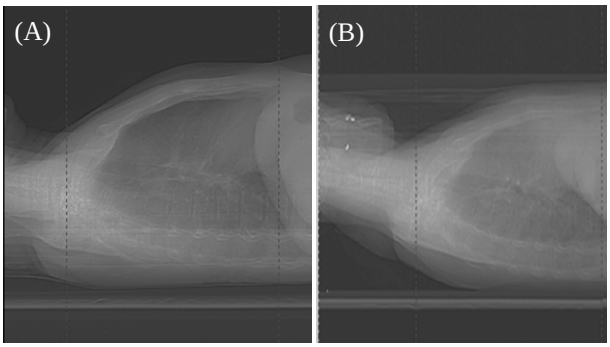

Figure 1. Example of lateral to pograms of a patient in inhalation (A) and exhalation (B) conditions, showing the length ranges of the reconstructed CT slices.

Biomechanical finite element modeling

The first step in the method of respiratory motion modeling used was to develop biomechanical FE models of the lungs and associated structures from the CT data in inhalation and exhalation conditions. The FE model of the thorax was governed in three steps [4]: (1) organ reconstruction, (2) soft-tissue properties assignment and (3) boundary condition definition.

Organ reconstruction

The radiologist contoured the lungs and thorax region for each patient for 3D reconstruction in the exhale stage images. The geometry of each patient in the exhale stage was then reconstructed from the DICOM images in a commercial medical image processing and editing software (MIMICS version 10.01, Materialise Company, Belgium) [15]. Each volumetric model was reconstructed using voxels, adding the information regarding the density of each material (defined in Hounsfield units) (figure 2). Since surface smoothing improved the quality of the surfaces for mesh generation in the FE model, this step was performed with five iterations in the MIMICS software. The smoothed 3D volumes were converted into a commercial FE method software package (ABAQUS version 6.8.1, Dassault Systems, Rhode Island, USA) for FE modeling [16]. As the accuracy of FE model is related to mesh density, by setting the global element size to 2 mm and using sufficiently fine mesh with tetrahedral elements, on average 10968 tetrahedral elements for each model, including all the organs, were used to minimize numerical errors. Meshing anatomical structures with tetrahedral elements was less challenging, as fewer tetrahedral were required to achieve a smooth surface [4, 16] (figure 3).

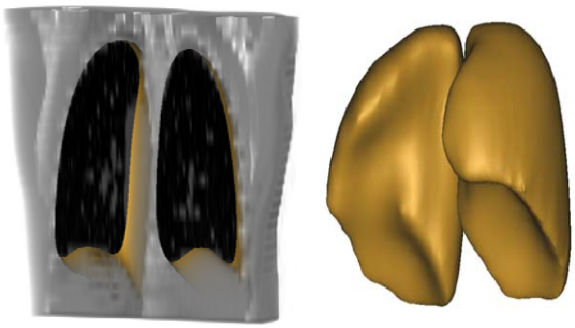

Figure 2. 3D reconstruction and segmentation of the organs, extracting the different organs from the CT image.

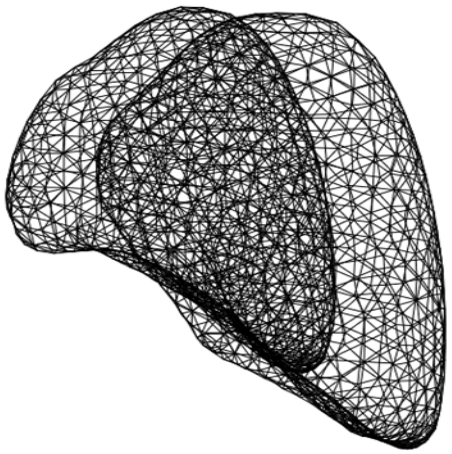

Figure 3. Finite element mesh of the lungs with 1728 nodes and 3448 elements in mesh.

Soft-tissue properties assignment

There was a significant variation in the material properties used to simulate the thorax region. A wide range of variation of the material properties of the different

tissues involved using different constitutive models have been reported in the literature [8, 9, 12, 17]. In this study, a simplistic model using linear elastic material properties was used, since nonlinear models significantly increase computation time, and complex patient-specific models are difficult to obtain for human tissues. The linear material properties were characterized by two parameters: Young's modulus, E, and Poisson's ratio, v. A larger Young's modulus indicates a stiffer material and a larger Poisson's ratio indicates a less compressible tissue [4]. The model parameters used for each organ are tabulated in table 2. The material properties were taken from the literature [9]. All elements belonging to the same organ were assigned the same material properties.

Table 2. Material properties used in modeling the thorax region.

	Young's modulus (E) kPa	Poisson's ratio (v)
Interior	6.0	0.40
Lung	5.0	0.45
Breast	19.0	0.45

Boundary condition definition

The contacts between organs and the supporting surrounding structures were defined. The organs' distension load and that from the surrounding structures were integrated into the boundary conditions. So, distension pressures (1.5-3 kPa depending on patient characteristic) for the lungs were exerted. As lung distension was the only cause of deformation of the thorax region, an internal pressure was uniformly applied on the inner lung wall to simulate an arbitrary lung deformation. The exact lung pressure corresponding to the known volume was unknown; however, since this model incorporated a linear system, the deformation caused by a different pressure could be calculated by scaling the results until the desired volume was reached.

Once the material properties, load and boundary conditions were defined, FE analysis was performed to determine the displacements of all nodes in the model. A dynamic explicit step was chosen for the FE analysis. The analysis was carried out on an Intel Duo Core CPU of 2.4 GHz with 4 GB of RAM and a 32 bits version of Windows XP.

Tuning and testing the model

One of the main goals of this work was to characterize the behavior of the tissues involved in the thorax using the deformation of the lungs between two different stages (inhalation and exhalation) in the simplest way. Once this behavior was determined for two patients, for achieving the deformation of known deformed thoraxes based on inhale and exhale CT images, the parameters of these three models were averaged and could be used to predict the deformation of a hitherto unknown thorax, having only the starting CT imaged geometry of the patient. These material properties were fitted using the information of the deformed thorax from the reference position (exhalation) and the final position (inhalation). Fitting of the material properties of the tissues involved was accomplished by using an FE model developed from the CT images of the patients.

The procedure for creating the geometric model from patient-specific CT data and our technique of FE-based lung motion modeling is summarized in figure 4. In order to tune the model parameters (to force the model to produce the changes observed between the inhale and exhale datasets), for three patients (patient 1, 2 and 3), the tissue mechanical properties, distension forces and boundary conditions were adjusted to find the optimum combinations of these parameters to individually produce the best match with CT images in both inhale and exhale stages. The parameters were fitted using the displacement of several landmarks located on the lung wall as characteristic points. Then, an average of the parameters for the above three test patients was taken to produce the model. Then, for the remaining three patients (patient 4, 5 and 6), the model with these

parameters was tested in a predictive mode in order to predict lung and thorax motion and deformation following respiration.

The images were analyzed for the magnitude of lung and thorax deformation relative to the baseline (exhalation) by measuring changes in distances between characteristic points. The positions of the different characteristic points considered by the radiologist are shown in figure 5. The way in which the distances between these points changed when the patient respired can be seen.

These points were also considered in the FE model. The new predicted location of these landmarks in the deformed lung, after inhalation, can be compared with the actual locations on the patient's CT images.

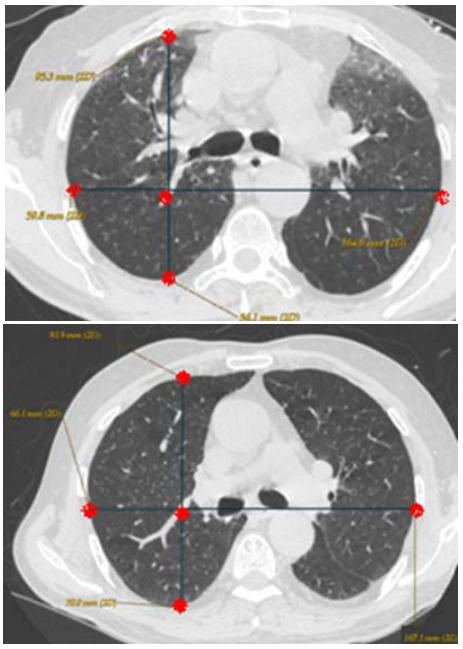

(A)

(B)

Figure 5. Landmark positions: inhalation (A) and exhalation (B).

Figure 4. A flow diagram of the modeling scheme showing the steps to convert CT images to an FE model.

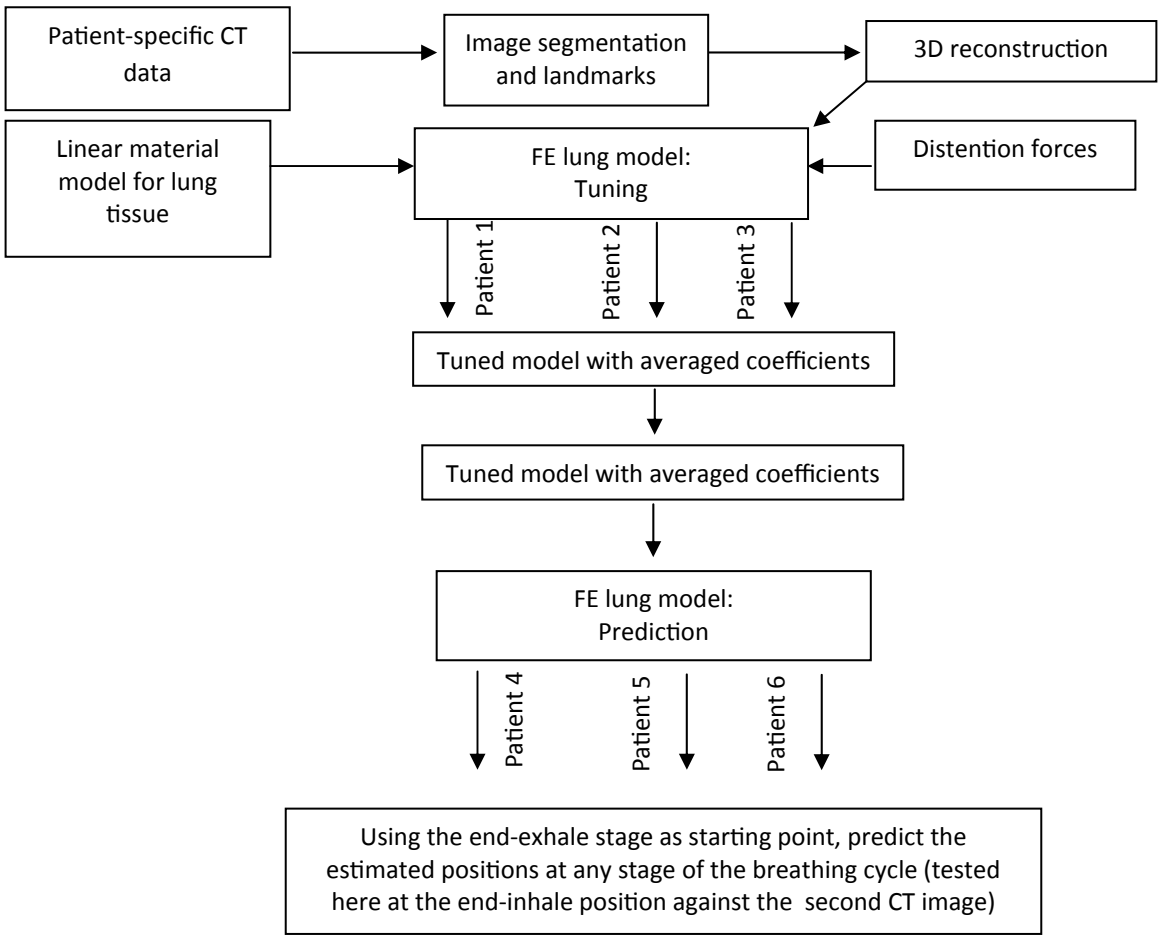

To tune the FE model, an iterative procedure varying the material properties, boundary conditions and deformation load was performed until the correct position of the landmarks in the deformed configuration was achieved.

As in the actual patient, the distances between the landmarks were measured and the parameters adjusted to minimize the discrepancy between the experimental measurements, and the displacement predictions. The objective function O_j was defined in terms of the sum of the squared residuals between the experimental and predicted results.

$$O_j = \sum_{i=1}^{N} [Di(Exp) - Di(FE)]^2 \qquad (1)$$

where, O is the cost function, j is the iteration number and "FE" and "EXP" represent FE analysis and experimental results, respectively.

The running process was stopped when the objective function satisfied the following criterion:

$$O_j \leq \Delta \qquad (2)$$

Δ being a prescribed specific limit value of patient n for the convergence [18]. Δ considered to be 1 mm for each patient. After calculating the average of the parameters, we applied those parameters on three tuned patients. to see if the following criterion is satisfied:

$$\sqrt{(\sum_{n=1}^{3}[\Delta p_n]\text{^}2)} \leq F \qquad (3)$$

Where Δp_n is sum of the squared residuals between the experimental and predicted results of patient n. In this study, F was considered 1 mm, as a specific limit value for the convergence.

RESULTS

The tuned thorax model for patients 1, 2 and 3 showed lung wall motion that matched the measurements from CT images within 1 mm. This means that by knowing the patient's anatomy in the exhale and inhale CT image, the model's parameters can be fine-tuned iteratively for the characteristic points in the model to start from exhale stage, apply the forces and reach within 1 mm of their corresponding points in the corresponding inhale stage.

Figure 6 illustrates the results of the prediction of lung deformation simulation in the coronal, sagittal and axial directions. Table 3 gives the mean local residual discrepancy related to the lung deformation in the predictive mode. In that mode, the maximum discrepancy between the landmarks and those predicted by the model were 9.4, 9.8 and 11.6 mm for patients 4, 5 and 6 respectively, while the mean discrepancy was 4.2 mm. The average computation time for each model in the fast predictive mode was 89 sec.

DISCUSSION

In this work, an approach has been presented to construct a 3D and fast lung respiration model that simulates lung deformation caused by respiration and predicts the lung deformation using only one patient CT image as input. Distance-based measures were used to assess the accuracy of the lung model.

The results of the tuning stage suggest that, provided that the model parameters are accurate, the model can potentially reach close agreement with reality in a predictive mode. In this study, we have evaluated the model only based on two stages of the breathing cycle (end-inhale and end-exhale). Starting from the image at the end-exhale stage for each specific patient, the FE model's parameters could be adjusted to reach the end-inhale stage with a discrepancy lower than 1 mm compared to that patient's CT image. The feasibility of doing this provided confidence to follow our next goal of finding a model for the fast prediction of lung deformation of other patients in a predictive mode.

Finding the optimized FE parameters of the first three patients enabled us to

Table 3. Distances between the landmarks in the inhale and exhale stages related to the lung deformation in the predictive mode (measurement vs. simulation).

			A (mm)	B (mm)	C (mm)	D (mm)	E (mm)	F (mm)	G (mm)
Exhale to inhale displace-	Patient 4	Measurement	5.4	17.5	10.2	9.4	6.8	9.2	7.3
		Simulation	7.2	8.1	12.8	11.3	7.9	3.8	13.3
	Patient 5	Measurement	5.8	17.1	15.3	10.6	13.9	15.4	10.9
		Simulation	3.4	7.3	15.9	5.8	8.3	7.1	14.6
	Patient 6	Measurement	6.1	18.4	17.8	11.1	15.7	15.5	13.2
		Simulation	3.1	6.8	14.2	7.5	8.6	6.8	15.7
	Average	Measurement	5.8 ± 0.3	17.7 ± 0.5	14.4 ± 3.1	10.3 ± 0.7	12.1 ± 3.8	13.4 ± 2.9	10.4 ± 2.5
		Simulation	4.6 ± 1.8	7.4 ± 0.5	14.3 ± 1.2	8.2 ± 2.3	8.3 ± 0.3	5.9 ± 1.5	14.5 ± 1.0
	Discrepancy (Measurement – Simulation)		1.2	10.3	0.1	2.1	3.8	7.5	4.1

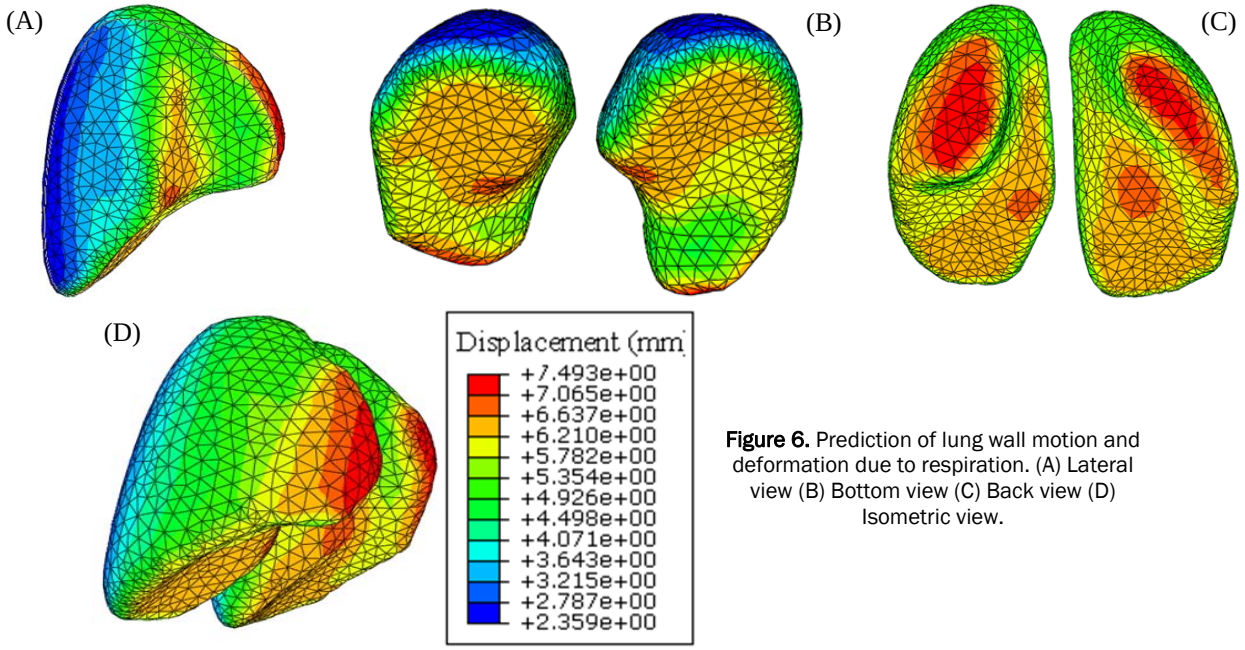

Figure 6. Prediction of lung wall motion and deformation due to respiration. (A) Lateral view (B) Bottom view (C) Back view (D) Isometric view.

develop our fast predictive model. Our results showed that, the model can predict respiratory lung motion with a mean discrepancy of about 4.2 mm, which is approximately comparable with the results of Brock *et al.* [9] and Al-Mayah [19].

In 2010, Jaesung *et al.* used nonlinear FE model, 4DCT data and measured pressure-volume data to perform predictive modeling of respiratory motion over the entire respiratory cycle [14]. They mentioned that the average differences of end-inspiration in the position between the landmarks and the prediction of the model for each patient were between 2 to 4.5 mm, while the computation time of each model was about 2.1 hours [14]. It is true that the Jaesung model shows lower discrepancy than our model, and it is clear that a more accurate model could be constructed using nonlinear material properties for the chest. However, in this paper, a faster way to assist the physicists to plan an intervention was achieved. In addition, incorporating other important structures in the chest such as ribs would also improve the accuracy of the model [5, 7], although that is expected to increase computation time. More recently, Mosleh-Shirazi *et al.* reported an FE model to predict prostate displacement and deformation due to bladder filling, rectal distension and patient posture during prostate brachytherapy [13]. However, most other studies applying FE on medical

images have mainly focused on single organ deformable registration [7-12]. For example, using FE, Bharatha *et al.* evaluated an image registration technique by defomable matching of preoperative images to improve the information content of intraoperative images [7]. In the thorax region, Zhang *et al.* proposed a lung model with pleural sliding which was implicitly validated by overlaying the CT lung image at inhalation and a reconstructed image of the lung at exhalation [12].

The accuracy of the lung model is highly correlated with the magnitude of lung volume change. The lateral and back parts of the lung showed larger discrepancies, especially when the lung deformation increased beyond 130% of the original volume. This was in good agreement with Zhang *et al.* who proposed a lung model using CT images of the inhalation and exhalation [12].

Considering the CT images, we observed that the increase in lung volume not only causes lung wall deformations, but also results in an interaction with all organs in the thorax region.

Our approach considered lung deformation as a mechanical process and simulated the deformations caused by respiration for the entire thorax. This made the FE method both more feasible and applicable to model lung deformation in radiotherapy.

The results of this study support the use of the FE simulation technique in future treatment planning systems to predict organ displacement and deformation, and to achieve accurate dose distributions throughout the implant volume.

One of the disadvantages of FE simulation in this study was the tuning time. The required calculation time for tuning the model was 88.6 hours (on a Pentium IV processor). This exceeds the time available in a clinical practice. However, this is a one-off simulation which was performed at the development stage of the model. The required calculation time for the fast model in the predictive mode was 89 sec. Therefore, by applying our fast predictive FE model before lung cancer radiotherapy, physicians and radiotherapist can have an approximate and fast view of the changes on their treatment planning system.

Ideally, evaluation of this model should be done by comparison with respiratory-correlated 4DCT images. We plan to carry out such a study next to fully evaluated the capabilities of this model, in particular, the intermediate stages between end-inhale and end-exhale in future.

CONCLUSION

The feasibility of developing a fast 3D FE model to simulate the interactions between chest organs caused by lung deformation due to respiration is demonstrated. This model shows promise for the prediction of approximate lung deformation, using just one image data set in the inhalation stage. This model can potentially help image-guided radiotherapy for lung cancer patients.

REFERENCES

1. Plathow C, Ley S, Fink C, Puderbach M, Hosch W, Schmähl A, Debus J, Kauczor HU (2004) Analysis of intrathoracic tumor mobility during whole breathing cycle by dynamic MRI. *Int J Radiat Oncol Biol Phys,* ***59****: 952-9.*
2. Langen KM and Jones DT (2001) Organ motion and its management. *Int J Radiat Oncol Biol Phys,* ***50****: 265–78.*
3. Ehrhardt J, Werner R, Frenzel T, *et al.* (2007) Analysis of Free Breathing Motion Using Artifact Reduced 4DCT Image Data. *Medical Imaging Proc SPIE,* ***6512****: 1N1-11.*
4. Bathe K (1996) Finite element procedures. Prentice-Hall, Englewood Cliffs.
5. Palomar AP, Calvo B, Herrero J, L´opez J, Doblar´e M (2008) A finite element model to accurately predict real deformations of the breast. *Medical Engineering & Physics,* ***30****:1089–97.*
6. Miga MI, Hoopes PJ, Kennedy FE, Hartov A, Roberts DW (2000) *In-vivo* modeling of interstitial pressure in the brain under surgical load using finite elements. *J Biomech Eng,* ***122****:354–63.*
7. Bharatha A, Hirose M, Hata N, Warfield SK, Ferrant M, Zou KH, *et al.* (2001) Evaluation of three-dimensional finite element-based deformable registration of pre- and intraoperative prostate imaging. *Med Phys,* ***28****:2551-60.*

8. Brock KK, Hollister SJ, Dawson LA, Balter JM (2002) Technical note: creating a four-dimensional model of the liver using finite element analysis. *Med Phys,* ***29****:1403-5.*
9. Brock KK, Sharpe MB, Dawson LA, Kim SM, Jaffray DA (2005) Accuracy of finite element model-based multi-organ deformable image registration. *Med Phys,* ***32****:1647-59.*
10. Liang J and Yan D (2003) Reducing uncertainties in volumetric image based deformable organ registration. *Med Phys,* ***30****:2116-22.*
11. Mohamed A, Davatzikos C, Taylor R (2002) A combined statistical and biomechanical model for estimation of intra-operative prostate deformation. 5th international conference on medical image computing and computer assisted intervention. *Lecture notes in computer science,* ***2489****:452–60.*
12. Zhang T, Orton NP, Mackie TR, Paliwal BR (2004) A novel boundary condition using contact elements for finite element deformable image registration. *Med Phys,* ***31****:2412-15.*
13. Mosleh-Shirazi MA, Faghihi R, Bagheri MH, Hadad K, Baradaran-Ghahfarokhi M. (2011) A finite-element model to predict prostate displacement and deformation due to bladder filling, rectal distension and patient posture during prostate brachytherapy. *Med Phys,* ***38****: 3553.*
14. Jaesung E, Xie GX, Suvranu D, Chengyu S (2010) Predictive modeling of lung motion over the entire respiratory cycle using measured pressure-volume data, 4DCT images, and finite-element analysis. *Med Phys,* ***37****:4389-400.*
15. Materialise Company. www.materialise.com/mimics.
16. Hibbit, Karlsson, Sorensen 2001 ABAQUS user's manual, v. 6.8: Pawtucket, RI, HKS Inc. USA.
17. Misra S, Macura KJ, Ramesh KT, Okamura AM (2009) The importance of organ geometry and boundary constraints for planning of medical interventions. *Medical Engineering & Physics,* ***31****: 195–206.*
18. Ruiter N, Muller T, Stotzka R, Gemmeke H, Reichenbach J, Kaiser WA (2002) Automatic image matching for breast cancer diagnostics by a 3D deformation of the mamma. *Biomed Tech,* ***47****: 644-7.*
19. Al-Mayah A, Moseley J, Brock K (2008) Contact surface and material nonlinearity modeling of human lungs. *Phys Med Biol,* ***53****, 305–317.*